

Method for direct observation of coherent quantum oscillations in a superconducting phase qubit. Computer simulations.

Ya. S. Greenberg

Novosibirsk State Technical University, 20 K. Marx Ave., 630092 Novosibirsk, Russia

(Dated: June 21, 2018)

Time-domain observations of coherent oscillations between quantum states in mesoscopic superconducting systems have so far been restricted to restoring the time-dependent probability distribution from the readout statistics. We propose a method for *direct* observation of Rabi oscillations in a phase qubit. The external source, typically in GHz range, induces transitions between the qubit levels. The resulting Rabi oscillations of supercurrent in the qubit loop are detected by a high quality resonant tank circuit, inductively coupled to the phase qubit. Here we present the results of detailed computer simulations of the interaction of a classical object (resonant tank circuit) with a quantum object (phase qubit). We explicitly account for the back action of a tank circuit and for the unpredictable nature of outcome of a single measurement. According to the results of our simulations the Rabi oscillations in MHz range can be detected using conventional NMR pulse Fourier technique.

PACS numbers: 03.65.Ta, 73.23.Ra

I. INTRODUCTION

As is known the persistent current qubit (phase qubit) is one of the candidates as a key element of a scalable solid state quantum processor.^{1,2} The basic dynamic manifestations of a quantum nature of the qubit are macroscopic quantum coherent (MQC) oscillations (Rabi oscillations) between its two basis states, which are differed by the direction of macroscopic current in the qubit loop.

Up to now Rabi oscillations in the time domain^{3,4} or as a function of the perturbation power⁵ have been detected indirectly through the statistics of switching events (e.g., escapes into continuum). In either case the probability $P(t)$ or $P(E)$ was obtained and analyzed to detect the oscillations.

More attractive is a direct detection of MQC oscillations through a weak continuous measurement of a classical variable, which would implicitly incorporate the statistics of quantum switching events, not destroying the quantum coherence of the qubit at the same time.^{6,7,8}

In this paper we describe an approach which allows a direct detection of MQC oscillations of macroscopic current flowing in a loop of a phase qubit. To be specific, we will use the example of three-Josephson-junction (3JJ) small-inductance phase qubit (persistent current qubit²) where level anticrossing was already observed.⁹

In our method a resonant tank circuit with known inductance L_T , capacitance C_T , and quality Q_T is coupled with a target Josephson circuit through the mutual inductance M (Fig. 1).

The method was successfully applied to a 3JJ qubit in classical regime¹⁰ when the hysteretic dependence of qubit energy on the external magnetic flux was restored in accordance to the predictions of Ref. 2.

Here we extend the approach which is described in our earlier paper.¹¹ We explicitly account for the back action of a tank circuit and for the unpredictable quantum mechanical nature of outcome of a single measurement.

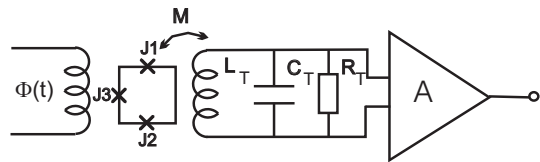


FIG. 1: Phase qubit coupled to a tank circuit.

According to the results of our simulations the Rabi oscillations in MHz range can be detected using conventional NMR pulse Fourier technique.

II. QUANTUM DYNAMICS OF 3JJ FLUX QUBIT

Quantum dynamics of this qubit has been studied in detail in Ref. 2. The qubit consists of a loop with three Josephson junctions. The loop has very small inductance, typically in the pH range. It insures effective decoupling of qubit from external environment. Two Josephson junctions have equal critical current I_c and capacitance C , while the critical current and capacitance of a third junction is a little bit smaller, αI_c , αC , where $0.5 < \alpha < 1$. If the Josephson coupling energy $E_J = I_c \Phi_0 / 2\pi$, where $\Phi_0 = h/2e$ is a flux quantum, is much more than the Coulomb energy $E_C = e^2/2C$, then the phase of a Cooper pair wave function is well defined. As was shown in Refs. 1,2 in the vicinity of $\Phi = \Phi_0/2$ this system has two quantum stable states with persistent circulating current of opposite sign. Therefore, the persistent current qubit can be described by following two-level Hamiltonian:

$$H_q = -\hbar(\varepsilon(t)\sigma_z + \Delta\sigma_x), \quad (1)$$

where σ_z and σ_x are Pauli spin operators.

Hamiltonian H_q is written in the flux basis: the basis of localized (left, right) states, so that two eigenvectors of σ_z correspond to the two classical states with a left or a right circulating current. Δ is the tunnel frequency and $\varepsilon(t)$ is in general a time dependent bias which is controlled by externally applied flux

$$\Phi(t) = \Phi_x + \Phi_{ac}(t), \quad (2)$$

where Φ_x is a time independent external flux, $\Phi_{ac}(t)$ is a monochromatic high frequency signal from the external source. According to (2) we write $\varepsilon(t)$ in the form:

$$\varepsilon(t) = \varepsilon_0 + \tilde{\varepsilon}(t). \quad (3)$$

In the absence of time dependent flux ($\tilde{\varepsilon}(t) = 0$) the eigenstates of Hamiltonian H_q are

$$E_{\pm} = \pm \hbar \Omega \equiv \pm \hbar \sqrt{\varepsilon_0^2 + \Delta^2}, \quad (4)$$

where $\varepsilon_0 = E_J f \lambda(\alpha, g) / \hbar$, $f = \Phi_x / \Phi_0 - \frac{1}{2} \ll 1$. The explicit dependence of $\lambda(\alpha, g)$ on qubit parameters α and $g = E_J / E_C$ has been found in Ref. 12. The flux states are the eigenstates of a macroscopic current which circulates in a qubit loop. Within a harmonic approximation¹² it is not difficult to find current operator in the flux basis: $\hat{I}_q = I_C(\lambda(\alpha, g) / 2\pi) \sigma_z$.

Hamiltonian H_q can be written in eigenstate basis as $H_q = -\hbar \Omega \sigma_Z$ with eigenfunctions Ψ_{\pm} : $H_0 \Psi_{\pm} = E_{\pm} \Psi_{\pm}$. The stationary state wave functions Ψ_{\pm} can be written as the superpositions of the wave functions in the flux basis Ψ_L, Ψ_R , where L, R stand for the left and right well respectively: $\Psi_{\pm} = a_{\pm} \Psi_L + b_{\pm} \Psi_R$,

$$a_{\pm} = \frac{\Delta}{\sqrt{2\Omega(\Omega \mp \varepsilon_0)}}, b_{\pm} = \frac{\varepsilon_0 \mp \Omega}{\sqrt{2\Omega(\Omega \mp \varepsilon_0)}}. \quad (5)$$

The transformation from flux basis to eigenstate basis is performed with the aid of rotation matrix $R(\xi) = \exp(i\sigma_Y \xi / 2)$, where $\cos \xi = \varepsilon_0 / \Omega$, $\sin \xi = \Delta / \Omega$. Therefore, the current operator in eigenstate basis is

$$\hat{I}_q = I_C \frac{\lambda(\alpha, g)}{2\pi \Omega} (\varepsilon_0 \sigma_Z - \Delta \sigma_X). \quad (6)$$

The high frequency excitation applied to the qubit induces the transitions between two levels which result in a superposition state for the wave function of the system: $\Psi(t) = C_+(t) \Psi_+ + C_-(t) \Psi_-$. The coefficients $C_{\pm}(t)$ can be obtained from the solution of time dependent Schrödinger equation with proper initial conditions for $C_{\pm}(t)$. From (6) we obtain the average current in the superposition state $\Psi(t)$:

$$\begin{aligned} \langle \Psi(t) | \hat{I}_q | \Psi(t) \rangle &= I_C \frac{\lambda(\alpha, g)}{2\pi} \frac{\varepsilon_0}{\Omega} (|C_-(t)|^2 - |C_+(t)|^2) \\ &\quad - I_C \frac{\lambda(\alpha, g)}{\pi} \frac{\Delta}{\Omega} \text{Re}(C_+(t) C_-^*(t)). \end{aligned} \quad (7)$$

Notice that at the degeneracy point ($f = 0$) the low frequency part of the average current, which is given by first term in (7), vanishes.

Below we define the density matrix elements $\rho_{00} = |C_-(t)|^2$, $\rho_{11} = |C_+(t)|^2$, $\rho_{10} = C_+(t) C_-^*(t)$, $\rho_{01} = \rho_{10}^*$, $\rho_{00} + \rho_{11} = 1$ which are related to spin operators: $\langle \Psi(t) | \sigma_Z | \Psi(t) \rangle = 2\rho_{00} - 1$, $\langle \Psi(t) | \sigma_X | \Psi(t) \rangle = 2\text{Re}\rho_{10}$, $\langle \Psi(t) | \sigma_Y | \Psi(t) \rangle = 2\text{Im}\rho_{10}$. We take the high frequency excitation in the form $\tilde{\varepsilon}(t) = \varepsilon_1 \cos(\omega t)$ and rewrite Hamiltonian (1) in the eigenstate basis Ψ_{\pm} :

$$H_q = -\hbar \left(\Omega + \frac{\varepsilon_0 \varepsilon_1}{\Omega} \cos(\omega t) \right) \sigma_Z + \hbar \frac{\varepsilon_1 \Delta}{\Omega} \cos(\omega t) \sigma_X. \quad (8)$$

From density matrix equation $i\hbar \dot{\rho}(t) = [H_q, \rho(t)]$ we get the following set of equations for the matrix elements of ρ :

$$\frac{dA}{dt} = 2 \frac{\Delta \varepsilon_1}{\Omega} \cos(\omega t) B, \quad (9)$$

$$\frac{dB}{dt} = -\frac{\Delta \varepsilon_1}{\Omega} \cos(\omega t) (2A - 1) - 2 \left(\Omega + \frac{\varepsilon_0 \varepsilon_1}{\Omega} \cos(\omega t) \right) C, \quad (10)$$

$$\frac{dC}{dt} = 2 \left(\Omega + \frac{\varepsilon_0 \varepsilon_1}{\Omega} \cos(\omega t) \right) B, \quad (11)$$

where $A = \rho_{00}$, $B = \text{Im}\rho_{10}$, $C = \text{Re}\rho_{10}$.

These equations cannot be solved analytically, however, we can try to predict the evolution of the quantities A, B, C since the Eqs. (9,10,11) are similar to those of a free spin in external magnetic field in NMR, where A is analogue of longitudinal magnetization M_Z , and B, C are analogues of transverse magnetizations M_Y and M_X , respectively. The only difference is that here the only detectable quantity is σ_Z component which is proportional to the circulating current. Therefore, we could expect the evolution of quantities A, B, C under the influence of external high frequency excitation is similar to that in NMR. If the frequency of external excitation ω is close to the gap frequency 2Ω , the main harmonic of A will be the Rabi frequency

$$\omega_R = \sqrt{(\omega - 2\Omega)^2 + \Omega_R^2}, \quad (12)$$

where Ω_R depends on qubit parameters and on the amplitude of excitation ε_1 , while the quantities B, C will oscillate with the gap frequency 2Ω , modulated by the Rabi frequency: $B, C \approx \sin \Omega_R t \sin 2\Omega t$. If $\varepsilon_1 \ll \Omega$ we can estimate Ω_R from Eqs. (9,10,11) in rotating wave approximation. We obtain

$$\Omega_R = \Delta \varepsilon_1 / \Omega. \quad (13)$$

Since we want here to treat the problem exactly we solved Eqs. (9,10,11) numerically.

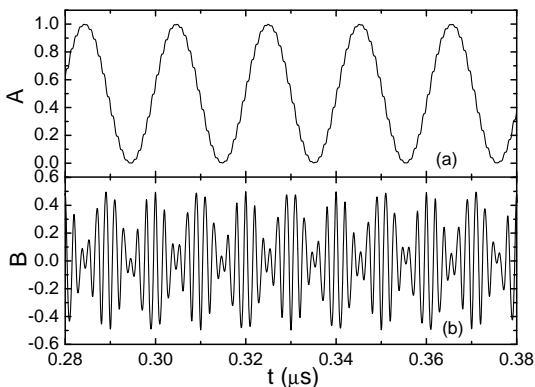


FIG. 2: Time evolution of A and B for qubit without dissipation.

For all computer simulations we take the following parameters of qubit: $I_C = 400$ nA, $L = 15$ pH, $\alpha = 0.8$, $g = 100$, $\Omega/2\pi = 250$ MHz, $\varepsilon_0 = \Delta$. The external high frequency is equal to the gap: $\omega = 2\Omega$. The excitation amplitude $\varepsilon_1 = 0.28\Omega$ which ensures the Rabi frequency $\Omega_R/2\pi = 50$ MHz. In addition, we assume the qubit is in its ground state in initial time $t_i = 0$, so that $A(0)=1$, $B(0)=C(0)=0$. In all simulations the time span is $10 \mu\text{s}$ from which the particular time windows had been choose for the figures.

The time evolution of $A(t)$ and $B(t)$ is shown on Fig. 2.

It is clearly seen that B oscillates with gap frequency, while the frequency of A is almost ten times smaller: (oscillation period of B : $T_B \approx 2 \times 10^{-9}$ s, while the same quantity for A is $T_A \approx 2 \times 10^{-8}$ s. The small distortions on A curve are due to a strong deviation of excitation signal from transverse rotating wave form, while B curve is clearly modulated with Rabi frequency Ω_R (Fig. 2).

The crucial requirement for the proper operation of a qubit is the preservation of phase coherence under influence of dissipative environment. We include the environment effects phenomenologically in Eqs. (9,10,11):

$$\frac{dA}{dt} = 2\frac{\Delta\varepsilon_1}{\Omega} \cos(\omega t)B - \frac{1}{T_r}(A - A_0), \quad (14)$$

$$\frac{dB}{dt} = -\frac{\Delta\varepsilon_1}{\Omega} \cos(\omega t)(2A-1) - 2\left(\Omega + \frac{\varepsilon_0\varepsilon_1}{\Omega} \cos(\omega t)\right)C - \frac{B}{T_d}, \quad (15)$$

$$\frac{dC}{dt} = 2\left(\Omega + \frac{\varepsilon_0\varepsilon_1}{\Omega} \cos(\omega t)\right)B - \frac{C}{T_d}, \quad (16)$$

where A_0 is the equilibrium value of density matrix $A_0 \equiv \rho_{00}^{eq} = \frac{1}{2}\left(1 + \tanh\frac{\hbar\Omega}{2k_B T}\right)$; T_r and T_d are relaxation and dephasing times, respectively. Here we have to consider density matrix elements as the quantities averaged over environments degrees of freedom: $A = \langle |C_-(t)|^2 \rangle$, $B = \text{Im}\langle C_+(t)C_-^*(t) \rangle$, $C = \text{Re}\langle C_+(t)C_-^*(t) \rangle$. The Eqs.

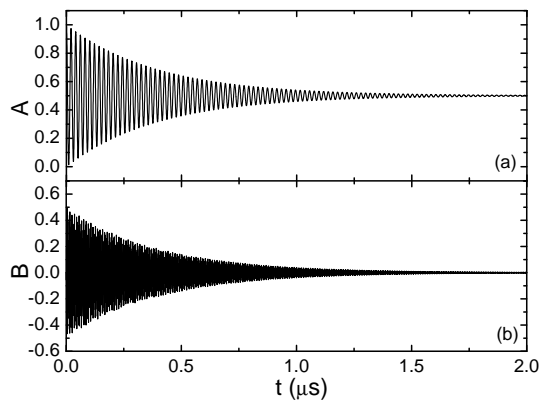


FIG. 3: Time evolution of A and B computed from Eqs. (14)-(16). $T_r = 50$ ms, $T_d = 200$ ns.

(14,15,16) are similar to well known Bloch-Redfield equations in NMR¹³.

For spin boson model of coupling of a qubit to thermal bath these times have been calculated for weak damping Ohmic spectrum by several authors (see^{14,15} and references therein). Here for estimations we take the expressions for T_r and T_d from¹⁶

$$\frac{1}{T_r} = \frac{1}{2} \left(\frac{\Delta}{\Omega}\right)^2 J(\Omega) \coth\left(\frac{\hbar\Omega}{2k_B T}\right), \quad (17)$$

$$\frac{1}{T_d} = \frac{1}{2T_r} + 2\pi\eta \left(\frac{\varepsilon_0}{\Omega}\right)^2 \frac{k_B T}{\hbar}, \quad (18)$$

where dimensionless parameter η reflects the strength of Ohmic dissipation. $J(\Omega)$ is the spectral density of the bath fluctuations at the gap frequency.

The decoherence is caused primarily by coupling of a solid state based phase qubit to microscopic degrees of freedom in the solid. Fortunately this intrinsic decoherence has been found to be quite weak¹⁷. However, the external sources of decoherence are more serious. Here we assume that the main source of decoherence is the external flux noise. For our computer simulations we take $T_r = 50$ ms, $T_d = 200$ ns¹¹. The evolution of A , B found from Eqs. (14,15,16) is shown in Fig. 3.

As is seen from the Fig. 3, A decays to 0.5 oscillating with Rabi frequency, while B (C) decays to zero. (Note: to be rigorous, the stable state solution for A is¹³

$$A \approx \frac{1}{2} + \frac{\rho_{00}^{eq}}{2(1 + \Omega_R^2 T_r T_d)}. \quad (19)$$

However, as distinct from conventional NMR where $\Omega_R^2 T_r T_d \approx 1$, for our values of Ω_R , T_r and T_d we get $\Omega_R^2 T_r T_d \approx 10^7$. For the same reason the stable state oscillations of B and C are quite small). It means the qubit density matrix becomes the statistical mixture: $\rho_{00} \rightarrow 1/2$, $\rho_{11} \rightarrow 1/2$, $\rho_{10} = \rho_{01} \rightarrow 0$ at $t \rightarrow \infty$. Therefore, the noise from environment leads to a delocalization: the system which initially is localized in any state would be always delocalized at $t \rightarrow \infty$.

This property has been first pointed out in connection with noninvasive measurements of coherent dynamics in quantum-dot systems¹⁸ where one can find an interesting discussion of how this behavior is related to the quantum Zeno effect, and recently has been confirmed for a quantum-dot qubit interacting with an environment and continuously monitored by a tunnel-junction detector¹⁹.

As is seen from Eq. 7), the delocalization leads to the vanishing of the current in the qubit loop.

III. THE MEASURING OF FLUX QUBIT WITH A TANK CIRCUIT

Below we consider a continuous measurements of a qubit with a classical tank circuit which is weakly coupled to the qubit via mutual inductance M . First we study the ideal case when qubit and tank circuit are completely decoupled from their environments, so that we may describe qubit + tank system by Hamiltonian $H = H_q + H_T + H_{int}$, where

$$H_T = \frac{Q^2}{2C_T} + \frac{\Phi^2}{2L_T}. \quad (20)$$

In (20) C_T , and L_T are capacitor and inductor of a tank circuit; Q is the charge at the capacitor, Φ is the magnetic flux trapped by the inductor. The tank-qubit interaction is described by Hamiltonian

$$H_{int} = \lambda \hat{I}_q \Phi, \quad (21)$$

where qubit current operator \hat{I}_q is given in (6), $\lambda = M/L_T$.

The equations for qubit + tank system are

$$\frac{dA}{dt} = 2 \frac{\Delta \varepsilon_1}{\Omega} \cos(\omega t) B - 2\lambda \eta I_C \frac{\Delta}{\hbar \Omega} B \Phi, \quad (22)$$

$$\begin{aligned} \frac{dB}{dt} = & -\frac{\Delta \varepsilon_1}{\Omega} \cos(\omega t) (2A - 1) - \\ & 2 \left(\Omega + \frac{\varepsilon_0 \varepsilon_1}{\Omega} \cos(\omega t) \right) C + \\ & 2\lambda I_C \frac{\eta}{\hbar \Omega} (2\varepsilon_0 C + \Delta(2A - 1)) \Phi, \end{aligned} \quad (23)$$

$$\frac{dC}{dt} = 2 \left(\Omega + \frac{\varepsilon_0 \varepsilon_1}{\Omega} \cos(\omega t) \right) B - 2\lambda \eta I_C \frac{\varepsilon_0}{\hbar \Omega} B \Phi, \quad (24)$$

$$\frac{d\Phi}{dt} = \frac{Q}{C_T}, \quad (25)$$

$$\frac{dQ}{dt} = -\frac{\Phi}{L_T} - \lambda \eta I_C F[\xi(t)], \quad (26)$$

where $\eta = \frac{\lambda(\alpha, g)}{2\pi}$. The function $F[\xi(t)]$ in (26) stands for stochastic nature of the measuring process. In accordance with von Neumann postulate the outcome of a single measurement cannot be predicted deterministically. When qubit is in a superposition of two stationary states its wave function $\Psi(t)$ can be expressed in the flux basis as $\Psi(t) = U\Psi_L + W\Psi_R$ where

$$|U|^2 = a_+^2 + A(a_-^2 - a_+^2) + 2Ca_+a_-, \quad (27)$$

$$|W|^2 = b_+^2 + A(b_-^2 - b_+^2) + 2Cb_+b_- \quad (28)$$

with $|U|^2 + |W|^2 = 1$.

The states Ψ_L, Ψ_R have equal currents circulating in opposite directions so that the outcome of the measurement (the direction of a current circulation) can be predicted only statistically with probability $|U|^2$ or $|W|^2$, respectively. Following this reasoning we take $F[\xi(t)]$ in the form:

$$F[\xi(t)] = \frac{|U|^2 - \xi(t)}{||U|^2 - \xi(t)|}, \quad (29)$$

where $\xi(t)$ generates random numbers from interval $[0, 1]$. Since $|U|^2 \leq 1$ the function $F[\xi(t)]$ takes two values: $+1, -1$. It accounts for unpredictable nature of a single measurement. If, for example, in some moment t_i $|U(t_i)|^2 > 0.5$ it is more probable to find the clockwise than counterclockwise direction of circulating current at this moment of time in a single measurement. The actual value of the voltage across the tank at some time t_i is obtained as the average of individual measurements over N different realizations of $\xi(t)$:

$$V(t_i) = \frac{1}{NC_T} \sum_{j=1}^{j=N} Q(t_i, \xi_j). \quad (30)$$

Therefore, our model accounts for stochastic back action influence of the measuring device (tank circuit) on the qubit behavior. In some sense the model resembles the probabilistic measurement scheme described in^{7,20} for detection of the electron position in double quantum dot by measuring the current through tunnel junction coupled to quantum double dot qubit.

Below, the tank circuit parameters are $L_T = 50$ nH, $C_T = 200$ pF, so that the tank is tuned to 50 MHz. The inductive coupling to the qubit $M = 12.5$ pH that gives for the coupling parameter $\lambda = 2.5 \times 10^{-4}$. In addition, we take $\varepsilon_0 = \Delta$ so that

$$|U|^2 = \frac{1}{\sqrt{2}} \left(\frac{\sqrt{2} + 1}{2} - A + C \right). \quad (31)$$

The results of computer simulations of the equation set (22,23,24,25, 26) are shown in Figs 4 and 5.

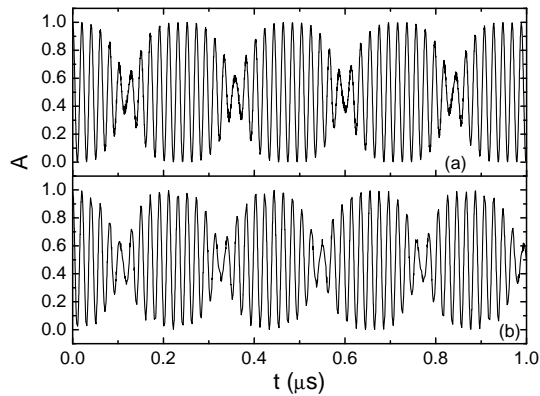


FIG. 4: Phase loss-free qubit coupled to a loss-free tank circuit. Oscillations of A . Deterministic case (a) together with one realization (b) are shown. Small scale time oscillations correspond to Rabi frequency.

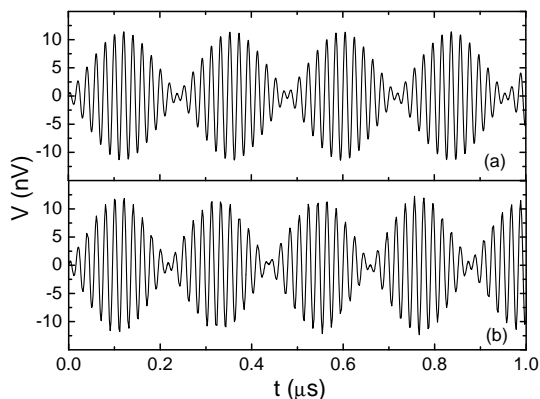


FIG. 5: Phase loss-free qubit coupled to a loss-free tank circuit. Voltage across the tank. Deterministic case (a) together with one realization (b) are shown.

At every graph of the figures the results for one realization of random number generator $\xi(t)$ are compared with the case when we replaced $F[\xi(t)]$ in (26) with deterministic term $(2A - 1 - 2C)/\sqrt{2}$, which means that the tank measures the average current (7) in a qubit loop. As is seen from the Fig. 4, A oscillates with Rabi frequency. The voltage across tank circuit oscillates also with Rabi frequency which is equal to 50 MHz in our case (Fig. 5) which is modulated with the lower frequency the value of which is about 5 MHz.

It is worth to note the interesting feature of the result: though the system is free from dissipation the voltage across the tank is not saturated (the voltage amplitude is about 10 nV, Fig. 5). Although A oscillates at resonance frequency of the tank, the saturation is not reached. A simple estimations show that at the tank resonance the saturated value of the voltage is about 75 nV. We have found the effect is due to the large value of a coupling constant λ . The simulations show the full saturation is reached with $\lambda \approx 10^{-8}$, however, then the voltage is quite small to be detected. These results are valid exactly for

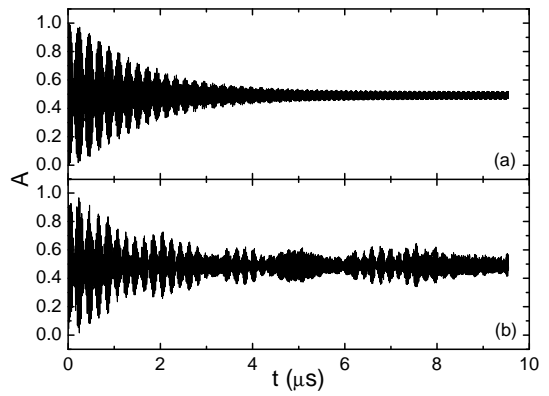


FIG. 6: Phase loss-free qubit coupled to a dissipative tank circuit. The evolution of A exhibits modulation of Rabi oscillations with lower frequency. Deterministic case (a) together with one realization (b) are shown.

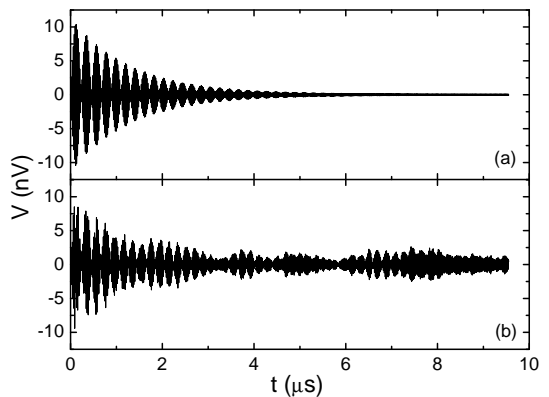


FIG. 7: Phase loss-free qubit coupled to a dissipative tank circuit. The voltage across the tank exhibits modulation of Rabi frequency. Deterministic case (a) together with one realization (b) are shown.

loss-free tank circuit, however we may within simulation time span (10 μs) extrapolate them for tank with high quality factor, say $Q_T > 1000$.

Now we want to account for the damping in the tank circuit. We replace Eq. 26 with

$$\frac{dQ}{dt} = -\frac{\Phi}{L_T} - \frac{\omega_0}{Q_T}Q - \lambda\eta I_C F[\xi(t)]. \quad (32)$$

For the simulations we take tank quality $Q_T = 100$. The results of simulations of equation set (22,23, 24, 25, 32) are shown for A in Figs. 6, and for the voltage in Figs. 7.

It is worthwhile to note that though the qubit is uncoupled from its own environment, nevertheless, the current in a qubit loop and the voltage across the tank decay. The quantities B and C which are not shown here oscillate without damping with the frequency of excitation with the amplitude equal to 0.5.

Finally, we consider the case when the qubit and the tank are coupled to their own environments. The corresponding set of equations are Eqs. (25,32) and following equations:

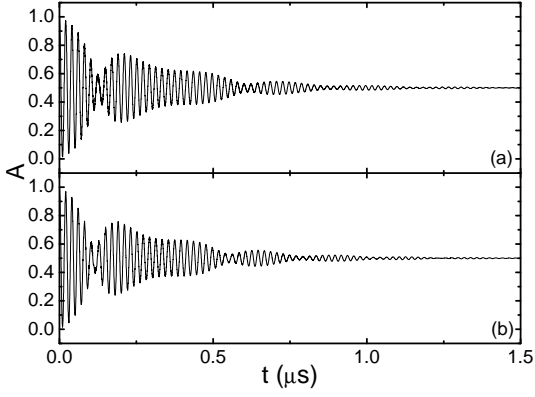


FIG. 8: Phase dissipative qubit coupled to a loss-free tank circuit ($1/Q_T = 0$). The evolution of A . Deterministic case (a) together with one realization (b) are shown.

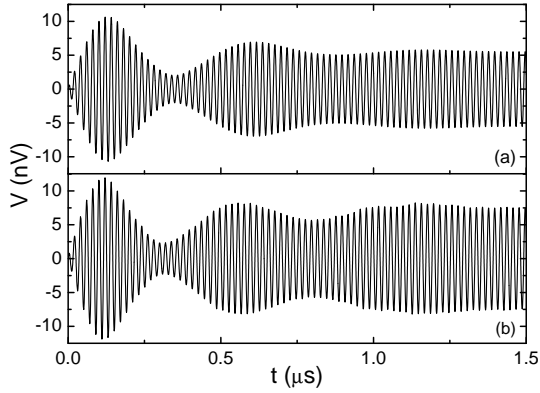


FIG. 9: Phase dissipative qubit coupled to a loss-free tank circuit ($1/Q_T = 0$). The voltage across tank circuit. Deterministic case (a) together with one realization (b) are shown.

$$\frac{dA}{dt} = 2 \frac{\Delta \varepsilon_1}{\Omega} \cos(\omega t) B - 2\lambda\eta I_C \frac{\Delta}{\hbar\Omega} B\Phi - \frac{1}{T_r}(A - A_0), \quad (33)$$

$$\begin{aligned} \frac{dB}{dt} = & -\frac{\Delta \varepsilon_1}{\Omega} \cos(\omega t)(2A - 1) - \\ & 2 \left(\Omega + \frac{\varepsilon_0 \varepsilon_1}{\Omega} \cos(\omega t) \right) C + \\ & 2\lambda I_C \frac{\eta}{\hbar\Omega} (2\varepsilon_0 C + \Delta(2A - 1))\Phi - \frac{B}{T_d}, \end{aligned} \quad (34)$$

$$\frac{dC}{dt} = 2 \left(\Omega + \frac{\varepsilon_0 \varepsilon_1}{\Omega} \cos(\omega t) \right) B - 2\lambda\eta I_C \frac{\varepsilon_0}{\hbar\Omega} B\Phi - \frac{C}{T_d}. \quad (35)$$

The results of simulations of the equation set (33,34,35,25,32) are shown in Figs. 8, 9, 10, 11, and Fig. 12.

From Fig. 8 and Fig. 10 we see that A is almost unaffected by the value of Q_T . Its decay is defined primarily by the shortest time T_d . The decay time of the voltage

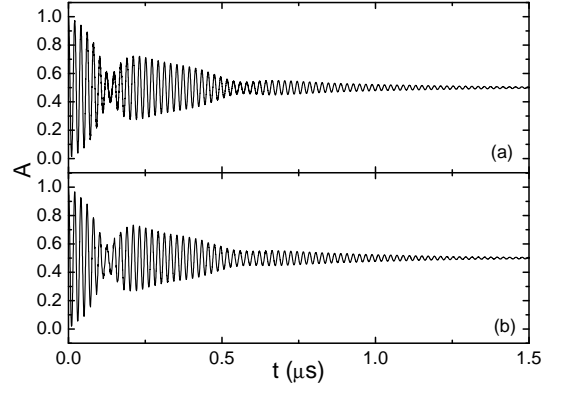


FIG. 10: Phase dissipative qubit coupled to a dissipative tank circuit ($Q_T = 100$). The evolution of A . One realization (lower graph) together with deterministic case (upper graph) are shown.

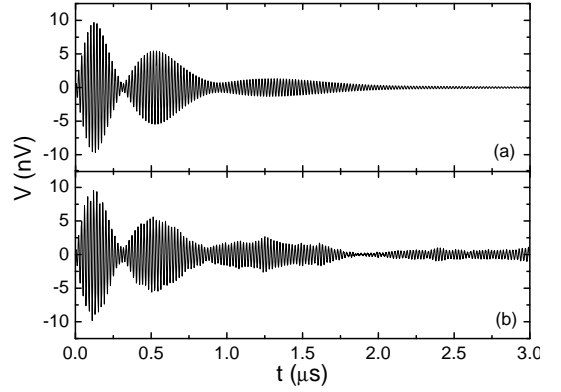


FIG. 11: Phase dissipative qubit coupled to a dissipative tank circuit ($Q_T = 100$). The voltage across tank circuit. One realization (lower graph) together with deterministic case (upper graph) are shown.

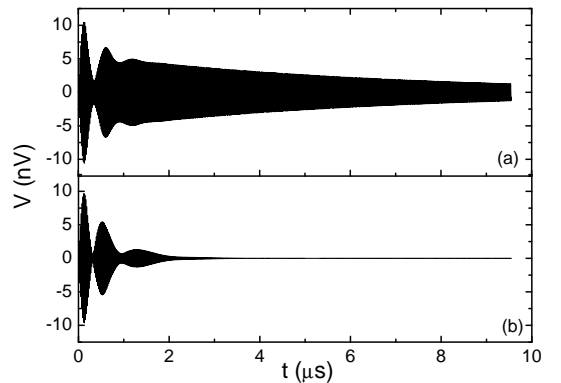


FIG. 12: Phase dissipative qubit coupled to a dissipative tank circuit. The voltage across the tank for deterministic case. Quality factors: $Q_T = 1000$ (upper graph) and $Q_T = 100$ (lower graph).

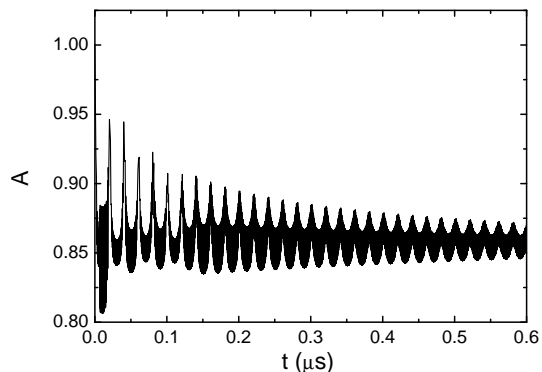


FIG. 13: Loss-free qubit coupled to a dissipative tank circuit ($Q_T = 100$), $\lambda = 2.5 \times 10^{-2}$. The evolution of A . A distance between neighbor jumps is equal to Rabi period. Deterministic case is shown.

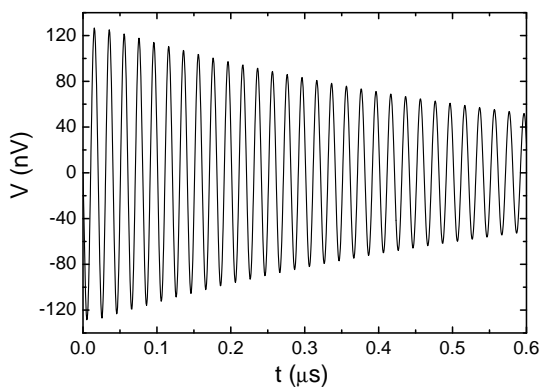


FIG. 14: Loss-free qubit coupled to a dissipative tank circuit ($Q_T = 100$), $\lambda = 2.5 \times 10^{-2}$. The evolution of the voltage across the tank for the deterministic case.

is defined by the value of Q_T , since tank circuit decay time $2Q_T/\omega_T$ is much longer than the dephasing time T_d (Figs. 9, 11, 12). It is advantageous from the point of experiment, since we can measure Rabi oscillations much longer than the dephasing time T_d . However, from the other hand, the maximum value of the voltage amplitude is almost independent of Q_T (see Fig. 12). We have shown in¹¹ that for carefully made electronics the voltage noise at the input of preamplifier could be on the order of 10 nV-20 nV. As is seen from Fig. 11 and especially, from Fig. 12, during the first microsecond the signal-to-noise ratio is about 0.5. The signal can be recovered with the well known in NMR pulsed technique with subsequent Fourier processing. However, since here the pulse filling frequency is uncoupled from the frequency of the signal to be detected, it is not necessary to keep the pulse width shorter than the decaying time of the signal. As our results show, the pulse duration of about 2 μs is adequate for the measurements.

In conclusion we want to show the effect of qubit evolution as the coupling between the qubit and the tank is increased. We numerically solved the system consisting of the loss-free qubit coupled to the dissipative tank cir-

cuit. The system is described by Eqs. (14,15,16,25) and Eq. (32). For the simulations we take the coupling parameter $\lambda = 2.5 \times 10^{-2}$. The results of simulations are shown on Figs. 13, 14 for deterministic case. As is seen from the Figs. 13 during Rabi period the quantity A became partially frozen at some level. At the endpoints of this period the system tries to escape to another level of A . Between the endpoints of Rabi period A oscillates with a high frequency which is about 10 GHz in our case. As expected, the evolution of B is suppressed approximately by a factor of ten below its free evolution amplitude which is equal to 0.5. As we show below, the strong coupling completely destroys the phase coherence between qubit states, nevertheless the voltage across the tank oscillates with Rabi frequency. Its amplitude is considerably increased and it does not reveal any peculiarities associated with the frozen behavior of A (Fig. 14).

IV. QUBIT WAVE FUNCTION

In conclusion we want to study the effect of a coupling between qubit and the tank on the qubit state, in particular, on phase coherence between basis states of the qubit. It is necessary to note that our *measurement* is not the *measurement* in the sense of Neumann. We are interested only in the voltage amplitude in the tank but not in the state of the qubit: we did not solve Schrodinger equations for $C_- = |C_-| \exp(i\varphi_-)$, $C_+ = |C_+| \exp(i\varphi_+)$ but for their products $A = |C_-|^2$, $B = |C_-||C_+| \sin(\varphi_+ - \varphi_-)$, $C = |C_-||C_+| \cos(\varphi_+ - \varphi_-)$. Nevertheless, we can check to what extent the qubit can be described by the wave function in case of its interaction with a tank. Evidently, free qubit must have definite wave function at any instant of time. It means the conservation of phase coherence the condition for which can be expressed in terms of our quantities as:

$$\frac{B^2 + C^2}{|C_-|^2 |C_+|^2} = 1. \quad (36)$$

If we switch on the interaction with a tank we may not, strictly speaking, consider qubit as having definite wave function. However, if the interaction is rather weak the qubit wave function could be well defined. We showed before that for relatively weak coupling the dissipation resulted in quenching A to the 0.5 level (see Figs. 6, 8, 10). That means $|C_+| = |C_-| \rightarrow \frac{1}{\sqrt{2}}$. However, as is seen from Fig. 15, the condition of phase coherence is still valid up to $\lambda \approx 10^{-3}$.

As the coupling is increased further the qubit wave function is completely destroyed. The quantity A is quenched to approximately 0.85 (Fig. 13). That is $|C_-| \approx 0.92$. It might seem that we have here so called Zeno effect- as if qubit state is frozen in its ground state. However, in case of a strong coupling it is not correct to say about wave function of the qubit alone. This is shown in Fig. 15 where for $\lambda > 10^{-2}$ the phase coherence is seen to be completely lost .

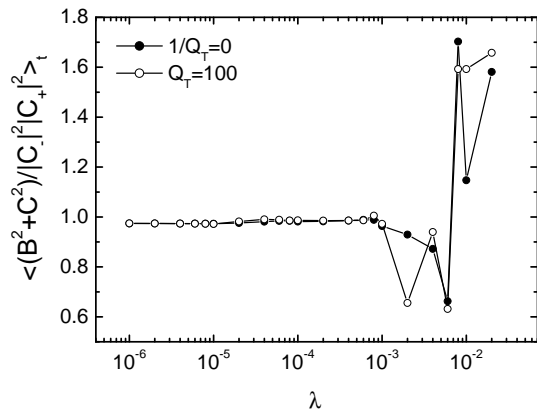


FIG. 15: The condition of phase coherence (36) vs coupling strength λ .

V. CONCLUSION

In all computer simulations we systematically compared different realizations with the case when we replaced $F[\xi(t)]$ in (26) with deterministic term $(2A - 1 - 2C)/\sqrt{2}$. We have found that within a decaying time all realizations and deterministic case give almost identical results. That is why in all corresponding graphs we compared deterministic case with the only realization. A clear difference appears only at the tails where A is close to 0.5 and C is rather small. This is because at the tails the random number generator every moment of time changes the sign of the current with a high probability, while within a decaying time where A undergoes oscillations the sign of the current for one half of period of oscillations of A is conserved with a high probability.

Throughout the paper we stress the similarity between the qubit+tank system and NMR, however, we have to be aware of the main difference. In NMR the back ac-

tion of the tank circuit on the sample under study is neglected. It is justified by the fact that the tank is coupled to macroscopic number of two-level systems (1/2-spin particles). The coupling to the individual particle is rather small, so that a reasonable signal level at the tank is obtained at the expense of enormous number of the coupled particles. However, when the tank is coupled to a single two-level system the account for back action is necessary. It leads to the main quantitative difference from NMR. In order to keep the noise from the tank as small as possible, the quality factor Q_T should be taken as high as possible from technological point of view (in our simulations we take $Q_T = 100$ only in order to save the simulation time). However, the signal amplitude weakly depends on Q_T being at best at the level of noise. Nevertheless, it is not difficult to recover the signal with the aid of the methods of signal processing which are used in high resolution NMR. Therefore, the results of our simulations clearly show that we can detect Raby oscillations of the voltage across tank circuit coupled to the qubit with the pulsed Fourier technique which is well known in NMR.

VI. ACKNOWLEDGEMENTS

I should like to express my gratitude to E. Il'ichev and M. Grajcar for many fruitful discussions on various experimental and theoretical aspects concerning the problems considered in the paper. I gratefully acknowledge A. Izmalkov for his help with computer simulations. I also want to express my appreciation to A. Maassen van den Brink for critical reading of manuscript and useful comments. The work was supported by INTAS Program of EU under grant 2001-0809.

- ¹ J. E. Mooij, T. P. Orlando, L. Levitov, L. Tian, C. H. van der Wal, and S. Lloyd, *Science* **285**, 1036 (1999).
- ² T. P. Orlando, J. E. Mooij, L. Tian, C. H. van der Wal, L. Levitov, S. Lloyd, and J. J. Mazo, *Phys. Rev. B* **60**, 15398 (1999).
- ³ Y. Nakamura, Y. A. Pashkin, and J. S. Tsai, *Nature* **398**, 786 (1999).
- ⁴ D. Vion, A. Aassime, A. Cottet, P. Joyez, H. Pothier, C. Urbina, D. Esteve, and M. H. Devoret, *Science* **296**, 886 (2002).
- ⁵ Y. Yu, S. Han, X. Chu, and Z. Wang, *Science* **296**, 889 (2002).
- ⁶ D. V. Averin, cond-mat/0004364.
- ⁷ A. N. Korotkov, *Phys. Rev. B* **63**, 115403 (2001).
- ⁸ A. N. Korotkov and D. V. Averin, *Phys. Rev. B* **64**, 165310 (2001).
- ⁹ C. H. van der Wal, A. C. J. ter Haar, F. K. W. R. N. Schouten, C. J. P. M. Harmans, T. P. Orlando, S. Lloyd, and J. E. Mooij, *Science* **290**, 773 (2000).

- ¹⁰ E. Il'ichev, T. Wagner, L. Fritzsche, J. Kunert, V. Schultze, T. May, H. Hoenig, H. Meyer, M. Grajcar, D. Born, et al., *Appl. Phys. Lett.* **80**, 4184 (2002).
- ¹¹ Y. S. Greenberg, A. Izmalkov, M. Grajcar, E. Il'ichev, W. Krech, and H.-G. Meyer, *Phys. Rev. B* **66**, 224511 (2002), cond-mat/0208143.
- ¹² Y. S. Greenberg, A. Izmalkov, M. Grajcar, E. Il'ichev, W. Krech, H.-G. Meyer, M. H. S. Amin, and A. M. van den Brink, *Phys. Rev. B* **66**, 214525 (2002), cond-mat/0208076.
- ¹³ A. Abragam, *The principles of nuclear magnetism* (Oxford University Press, Oxford, 1983).
- ¹⁴ A. J. Leggett, S. Chakravarty, A. T. Dorsey, M. P. A. Fisher, A. Carg, and W. Zwerger, *Rev. Mod. Phys.* **59**, 1 (1987).
- ¹⁵ U. Weiss, *Quantum Dissipative systems* (World Scientific, Singapore, 1999).
- ¹⁶ M. Grifoni, E. Paladino, and U. Weiss, *Eur. Phys. J.* **B10**, 719 (1999).

- ¹⁷ L. Tian, L. S. Levitov, C. H. van der Wal, J. E. Mooij, T. P. Orlando, S. Lloyd, C. J. P. M. Harmans, and J. J. Mazo, in *Quantum Mesoscopic Phenomena and Mesoscopic Devices in Microelectronics*, edited by I. Kulik and R. Ellialtıođlu (Kluwer, Dordrecht, 2000), p. 429.
- ¹⁸ S. A. Gurvitz, Phys. Rev. B **56**, 15215 (1997).
- ¹⁹ S. A. Gurvitz, L. Fedichkin, D. Mozysky, and G. P. Berman, cond-mat/0301409.
- ²⁰ A. N. Korotkov, Phys. Rev. B **60**, 5737 (1999).